0. Scope

This report covers the analysis of data taken during the Herschel STM2 straylight testing on the 19th and 20th October 2006 at ESTEC.

1. Test Configuration

The detailed test configuration for the Herschel STM-2 EPLM is reported elsewhere (AD1). Here we briefly outline the test setup to allow this report to be read alone.

- Herschel flight cryostat in its STM-2 configuration
  - Only the main Helium tank is filled and the covers are cooled via external dewars
  - The cryostat lid is closed and cooled via an external cooling loop
  - The cryostat lid is polished to give a low emissivity finish

- Instrument suite
  - The SPIRE CQM FPU is fitted – this has only the photometer long wavelength (PLW) array fitted. The CQM PLW is an engineering unit with non flight performance, in particular several detectors to not operate on this unit.
    They are: **B5 B6 A1 E1 E3 D5 D8**
  - The SPIRE QM2 warm electronics units were used to drive the FPU. These have near flight performance and full flight functionality.
  - The HIFI CQM unit is fitted but non-functioning. Only one optical channel is fitted – all other LOU ports are blocked within the cryostat.
  - The PACS STM unit is fitted which is a structural model only.

- External straylight source
  - An external radiation source is used to illuminate the LOU ports. In order to distinguish this source from the ambient background a chopper is employed in front of a Pegasus R hot black body source to allow post detection demodulation of the signal.
  - The external source was mounted on an external frame to allow illumination of different paths through the LOU and alignment windows – see figures 1-2.
  - A metal shield was placed in front of the source for protection which was used to define the “on” and “off” configurations for the source illumination – see figure 3.

Figure 1: The external radiation source mounted on its frame on the outside of the Herschel cryostat.

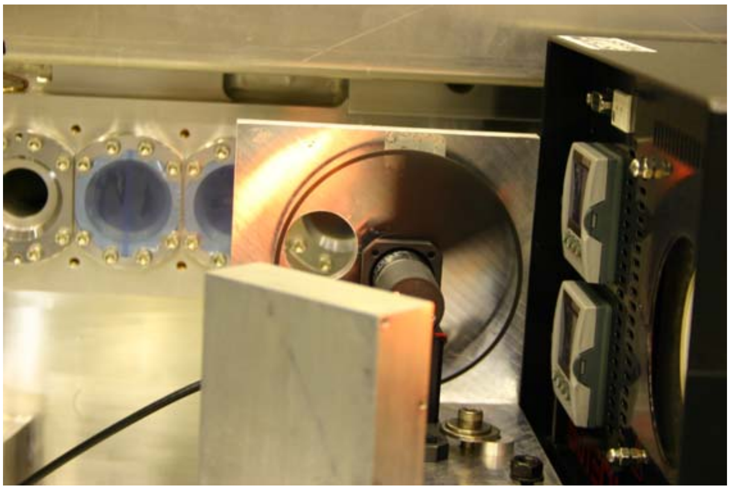

Figure 2: Close up of the external source showing the HBB aperture; the fold mirror and the chopper. The open LOU window can be seen through the defining aperture and the alignment window is seen to the far left.

Figure 3: Removing the protective shield in front of the external source. This shield covered all LOU and alignment ports and was used to define the “on” and “off” states for the test.

2. Test cases

Two basic types of test were carried out:

Static load tests – the cryostat was set to a pre-determined condition and a V-I or “loadcurve” was taken on the PLW bolometer which, once analysed, can be used to establish the temperature of the detectors and, therefore, estimate absorbed power.

External illumination tests – here the external chopped source was placed at various locations with respect to the LOU and alignment windows and the data from the detectors, set at nominal operating condition, were recorded

In addition to these tests, standard calibrator sequences (PCAL Flashes) were taken at regular intervals to monitor the basic response characteristics of the detectors. For each type of test I record here the test cases carried out and the unique **OBSID** used to identify the data in the HCSS database.

2.1 Static Tests

Table 1 lists the test dates and times and basic cryostat conditions. The actual temperatures are given in the next section under each case number.

Table 1: Cases for static tests

Case	Cryostat set up	Observation type	Date and time (UT)	OBSID
0	Cold during EMC test	SPIRE_STM2_LC_P	2006-10-18 08:22:16-08:54:26	B0000062
1	Cold start of straylight	SPIRE_STM2_LC_P	2006-10-19 08:53:33-09:25:43	B0000092
2	Cold shields before lid warmed up	SPIRE_STM2_LC_P	2006-10-19 14:54:25-15:26:34	B00000AD
3	Warm lid ~80 K	SPIRE_STM2_LC_P	2006-10-19 16:46:26-17:18:36	B00000B4
4	Hot lid ~ 197 K	SPIRE_STM2_LC_P	2006-10-20 05:18:46-05:50:56	B00000BF
5	Cold lid with warm shields	SPIRE_STM2_LC_P	2006-10-20 09:25:17-09:57:27	B00000C8

2.2 External Illumination Tests

Table 1 lists the test dates and times and basic cryostat conditions. The actual temperatures are given in the next section under each case number.

Table 2: Cases for external illumination tests

Case	Cryostat set up	Observation type	Date and time (UT)	OBSID
1	HBB centred on LOU band 3 port - this is Z_o	Chopped frequency 1.7 Hz	2006-10-19 11:00:55-11:19:11	B0000099
2	HBB moved Z_o+15 mm wrt LOU port	Chopped frequency 1.7 Hz	2006-10-19 11:37:09-11:55:42	B000009C
3	HBB moved Z_o+30 mm wrt LOU port	Chopped frequency 1.7 Hz	2006-10-19 11:59:16-12:18:36	B000009F
4	LOU port blocked with tape	Chopped frequency 1.7 Hz	2006-10-19 12:35:15-12:45:17	B00000A2
5	HBB centred on left alignment port	Chopped frequency 1.7 Hz 0.76 Hz 0.31 Hz 3.3 Hz	2006-10-19 13:11:07-13:50:40	B00000A6
6	HBB centred on right alignment port	Chopped frequency 3.3 Hz 1.74 Hz 0.25 Hz	2006-10-19 13:59:08-14:38:04	B00000A9

2.3 Calibration of gain

The basic voltage gain of the pre-amplifiers plus electronics units can be checked by plotting the signal on the broken (open) pixels versus the applied bias volts. Figure 4 shows the result with standard gain correction applied.

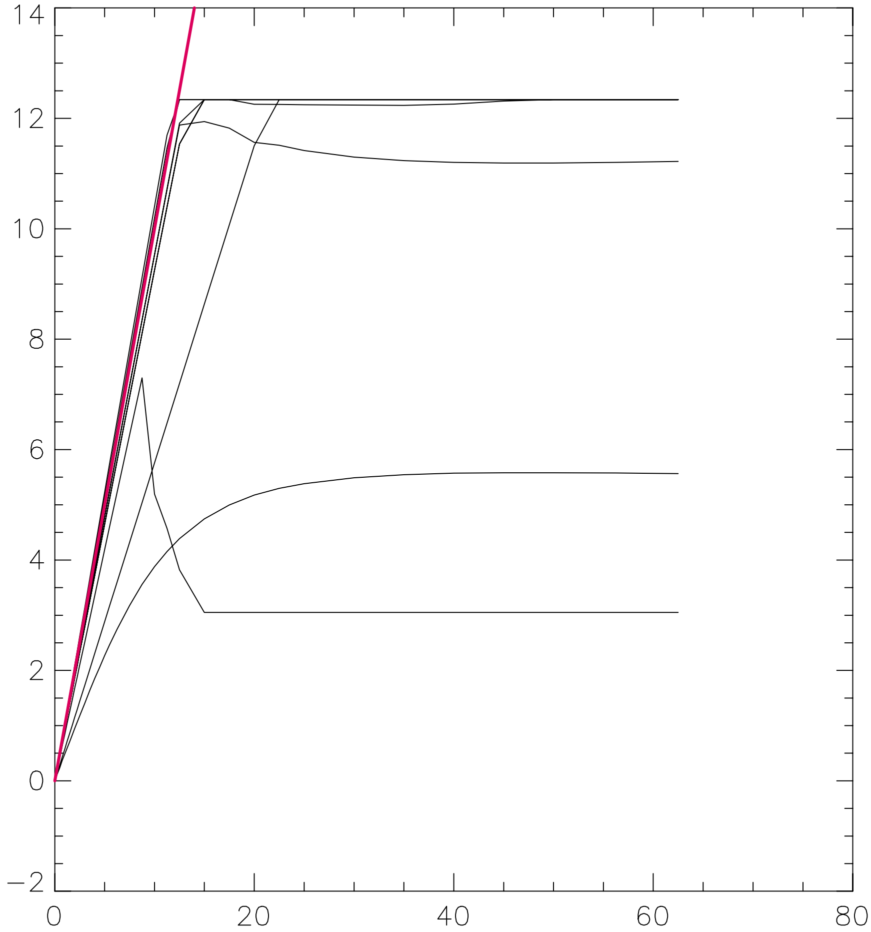

Figure 4: Open channel signal versus applied bias – both axes in mV. The red line represents 1:1 showing the applied gain correction is accurate.

2.4 PCAL Flash

As further check on the response of the system photometer calibrator (PCAL) flashes were carried out at various times over the period of the test campaign. I have analysed one flash (OBSID B0000098) as an example and to compare to the PCAL flashes carried out during the EQM testing – see figure 5. The general level of the response is about the same – between 0.02 and 0.03 pW - with a peak in the centre of the array as expected from the presence of the reflector on the cryostat lid. What is different for the STM-2 case is the enhanced signal across one row (A) of the detector – see also figure 6 . This reason for this is not entirely clear and further analysis will be required to assess how it arises. Also, during the EQM testing there was a very large ambient background on some detectors that suppressed their response to a high degree. This explains the anomalously large reported response for E2 and E4 in the upper plot of figure 5.

We should also compare these results with those from the CQM instrument testing. This will be added in a future version of the report; meanwhile, we can assume that the detector response is nominal for the purposes of evaluating the data from the STM-2 straylight and EMC testing.

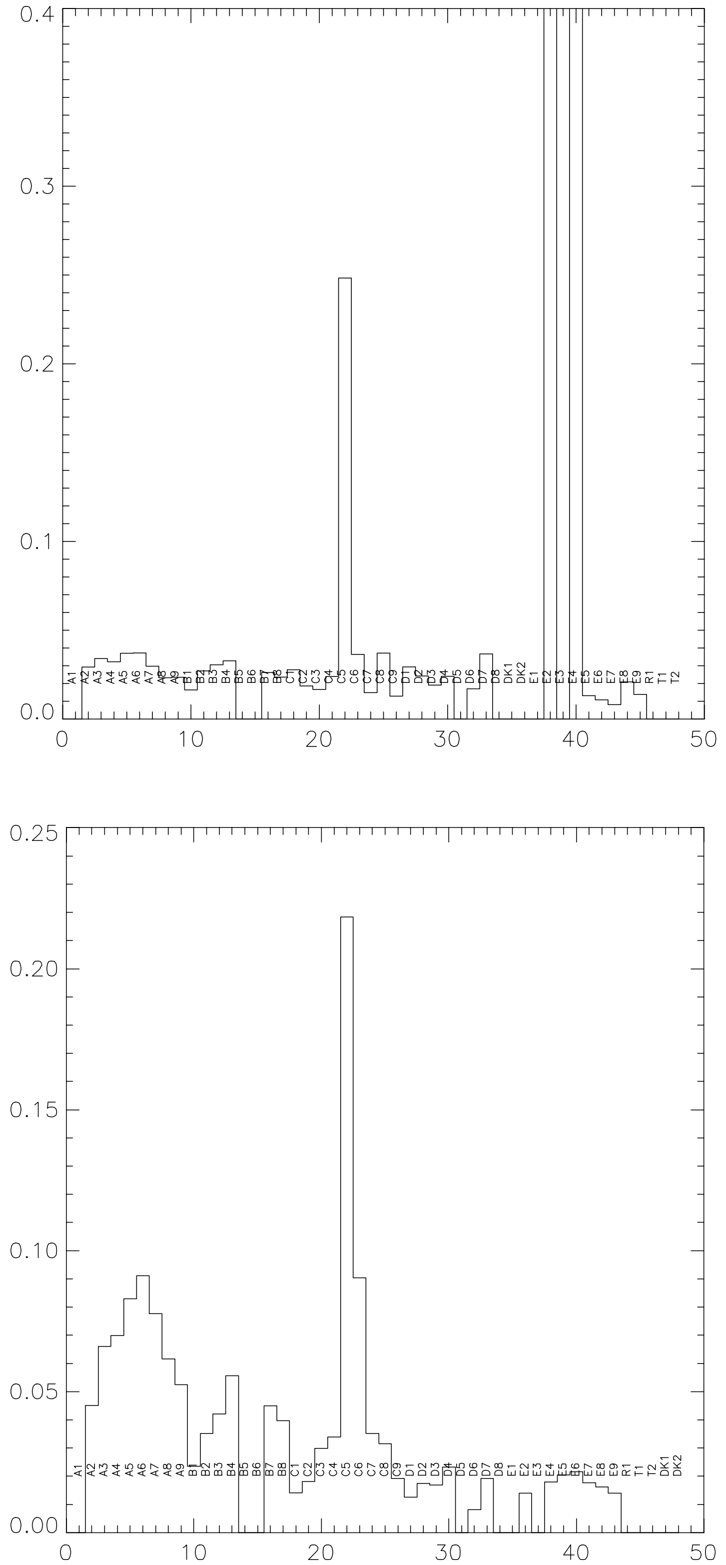

Figure 5: Estimated absorbed power on PLW for a PCAL flash during the EQM testing (upper) and during the STM-2 straylight testing (lower). The y-axis is pW in each case and the histogram represents each individual pixel as labelled.

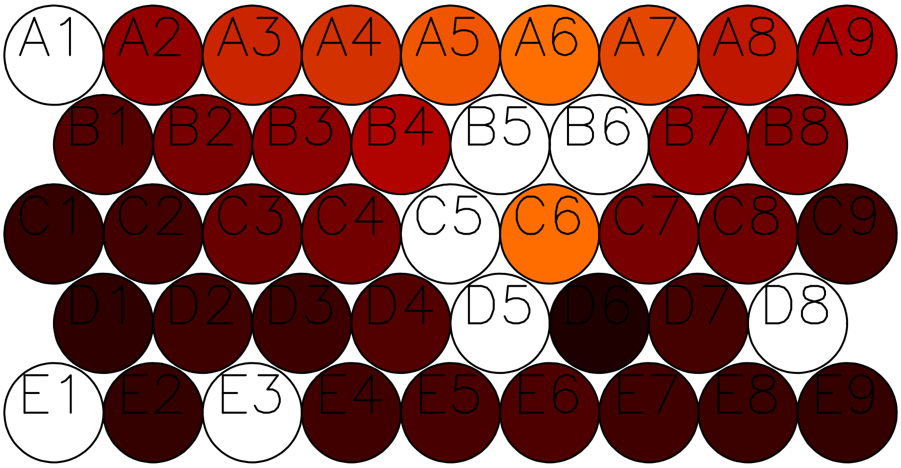

Figure 6: Distribution of power from a PCAL flash during the STM-2 test campaign. C5 is saturated in this image, all other "white" pixels are non-operational.

3 Test Case Results

3.1 Static Straylight

3.1.1 Method of determining absorbed optical power.

Using the data from two loadcurves, one a baseline and one during a particular measurement setup, one can estimate the additional absorbed optical power by one of three complementary, but separate, methods; all of which start by converting the measured current flowing through the thermistor to resistance. From the resistance and a predetermined calibration one can find the temperature of the thermistor. From the temperature we can estimate the thermal conductance of the bolometers, again using a predetermined calibration. Knowing the bias voltage and current gives the electrical power dissipated in the thermistor. From these parameters the optical power can be estimated by:

i) Taking the difference in applied electrical power at a given temperature between the two loadcurves. This method is accurate if the optical power is reasonably large compared to the electrical power and the sink temperature is the same during the two measurements.

ii) Taking the zero electrical power (low bias) temperature difference for each bolometer between the baseline and the measurement case and using the derived thermal conductance to estimate the total power. The optical power is then given by subtracting the electrical power.

iii) Calaculating the total power for the baseline and measurement case in turn using the temperature difference between each pixel and the sink as measured by thermistors directly mounted to the sink. The difference between the total power then gives the additional power for the measurement case (assumed to be the additional optical load)

All three methods are reported in what follows – please note the caveat on method (i)

3.1.2 Case 0,1,2: Everything cold

I take as reference here the loadcurve OBSID B0000092 – first LC taken on 19th October – and compare with OBSID B00000AD taken just before warming the lid up. The results were the same when using the loadcurve OBSID B0000062 taken under cold conditions the previous day. Figure

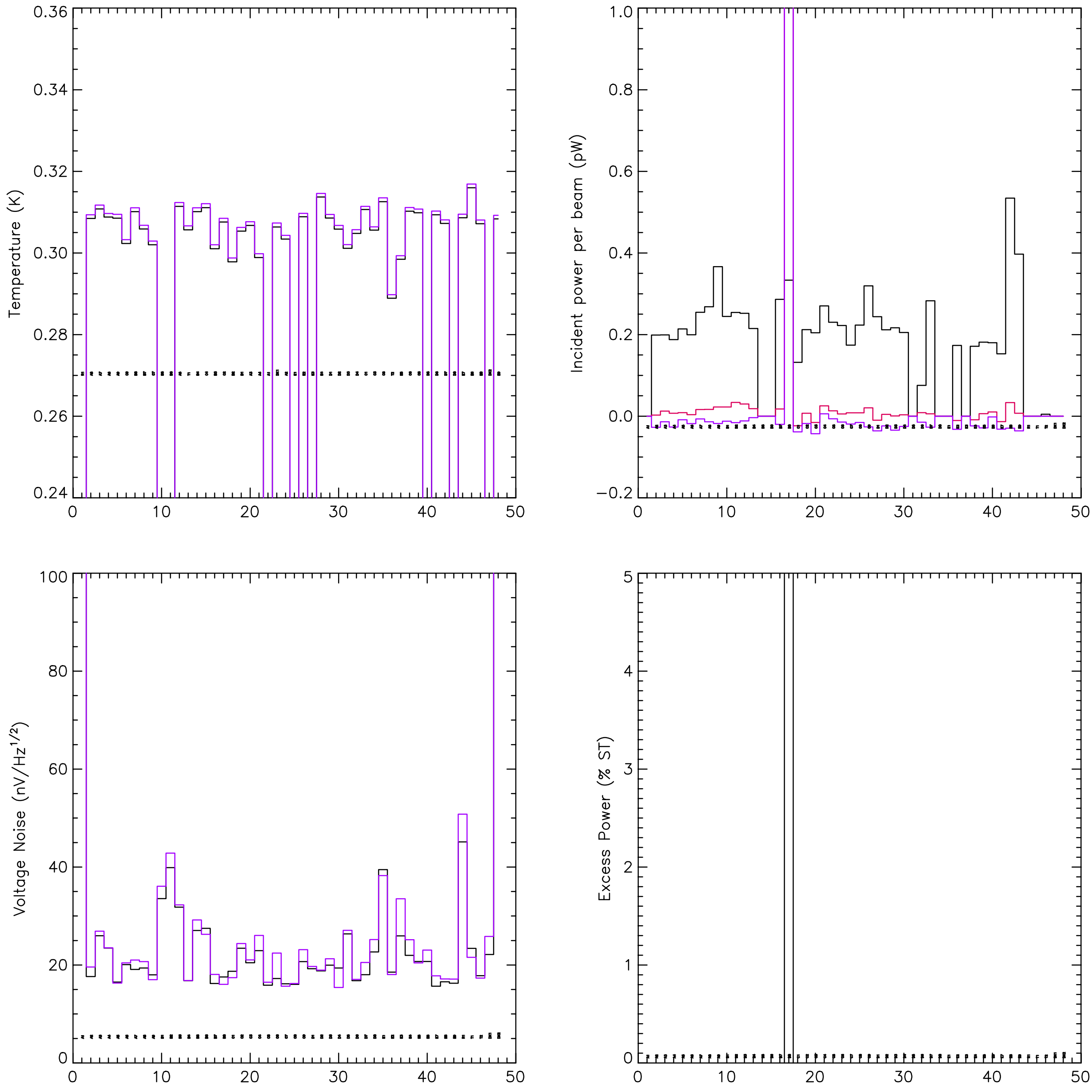

Figure 7: Results for Case 1/Case 2 comparison.
Upper left: Temperature. Case 1 black; Case 2 Purple.
Upper right: Estimated incident power on SPIRE calculated by the three methods described in the text. (i) Black; (ii) Red; (iii) Purple.
Lower left: Voltage noise at standard bias – Case 1 black; Case 2 Purple
Lower right: Incident power on SPIRE expressed as percentage of the "standard telescope". Here the absorbed power is taken as essentially zero.

7 shows the results. In order to express the optical power in the units used in the straylight modelling I have first referred the absorbed power to the entrance aperture of SPIRE and then divided by the power that would be incident on the aperture from the "standard" telescope. This is taken as being a surface that fills the beam with a temperature of 70 K and an emissivity of 1.5%, the same as used in the ASAP model calculations reported in the spreadsheet

TSE_Herschel_STM2. Pixel B8 seems to give a large signal but inspection of the temperatures does not support the result, further investigation of the data are required – again for a future version of this note.

The discrepancy between the absorbed power estimates demonstrates a) the somewhat unreliable nature of the loadcurve power comparison for small powers and b) that the optical power is not measurable by DC comparison of the temperature to better than ~±0.02 pW with our current knowledge of the detector calibration.

I take as a working assumption that in the cold case the in band optical power inside the cryostat in negligible.

3.1.3 Case 3: Lid at 80K

A loadcurve was taken at 16:44 when lid was about 80 K (OBSID B00000B4). The actual temperature of the lid and shields during the measurement is shown in figure 8. In order to make the results as accurate as possible I have fitted the lid (PT1000_SPARE1) data and used the fit to generate the temperature of the lid at each point in the load curve. This means the estimate of the contribution from the lid can be assessed much more accurately. Figure 9 gives the results in the same format as for Case 1 except here the excess power is taken as the optical power incident on the SPIRE aperture excluding the estimated contribution from the lid (see appendix for how this was calculated). This power therefore represents the “stray” light that cannot be explained by the load from the mirrored reflector filling the beam. Note here that the two temperature based methods of estimating the power now agree.

Figure 10 shows the distribution of the straylight across the array. As with the PCAL flash row A (and possibly row E) appears to show increased straylight compared to the average across the array. Pixel B8 again gives an anomalous result for the power, unsupported by the temperature calculation.

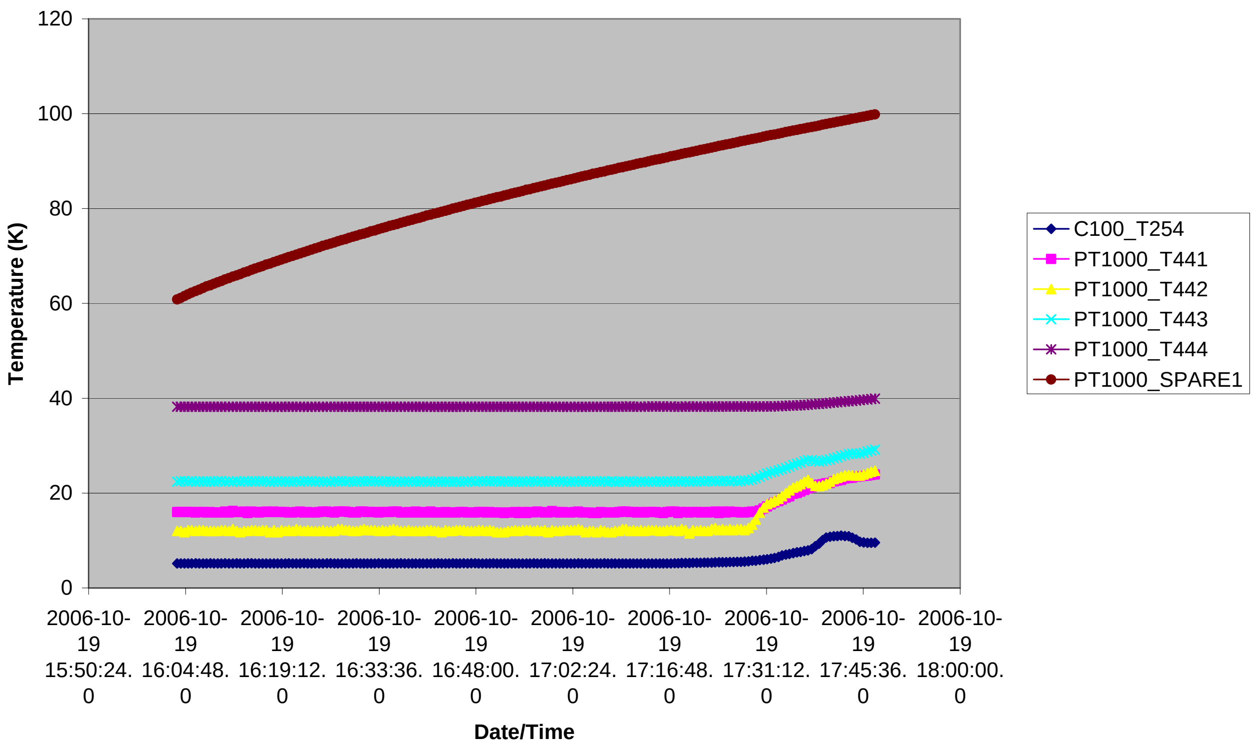

Figure 8: Lid and shield temperatures during case 3.

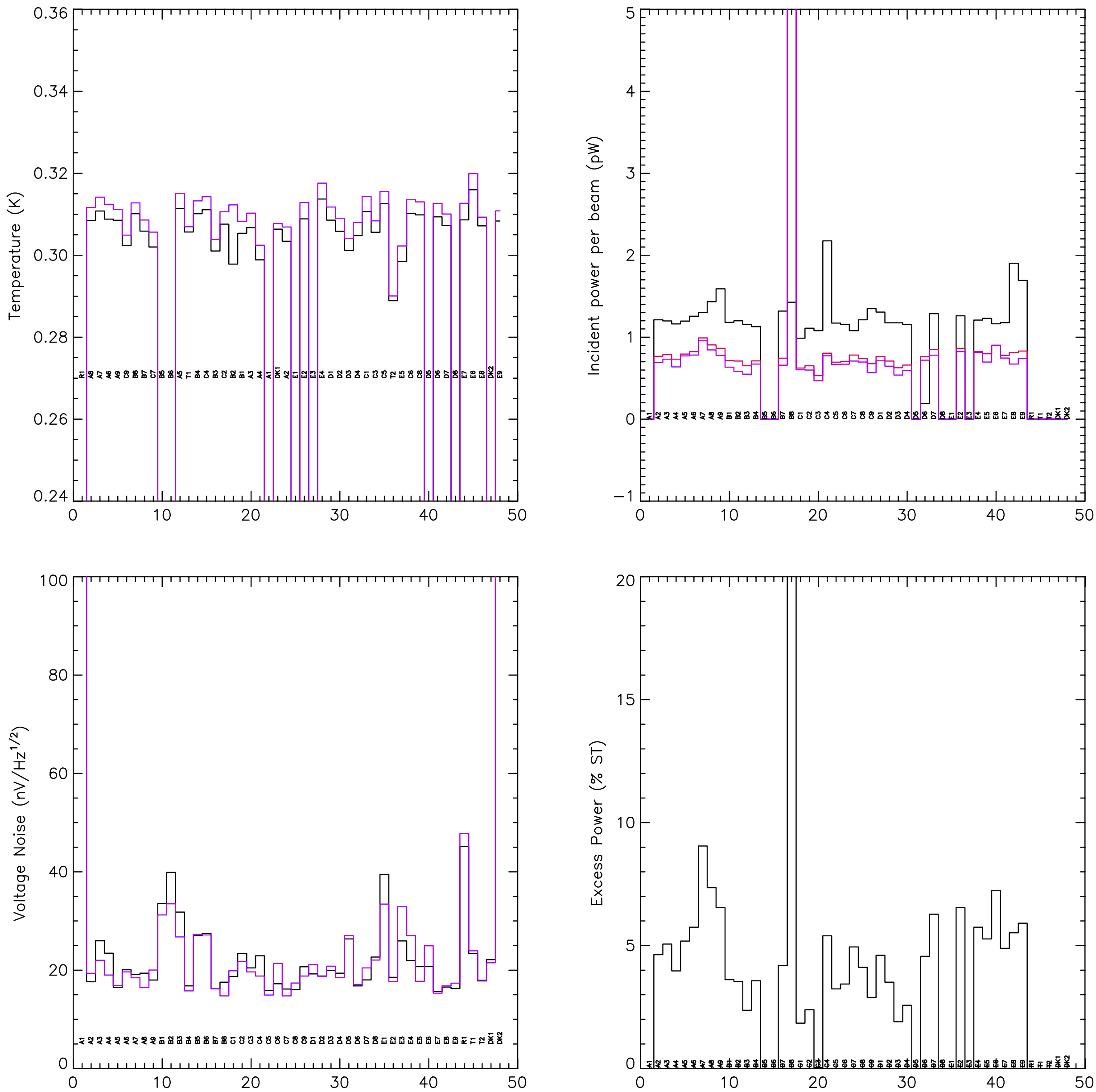

Figure 9: Results for Case 3/Case 2 comparison.

Upper left: Temperature. Case 2 black; Case 3 Purple.

Upper right: Estimated incident power on SPIRE calculated by the three methods described in the text. (i) Black; (ii) Red; (iii) Purple.

Lower left: Voltage noise at standard bias – Case 2 black; Case 3 Purple

Lower right: Excess incident power on SPIRE over and above that from the mirrored lid expressed as percentage of the “standard telescope”.

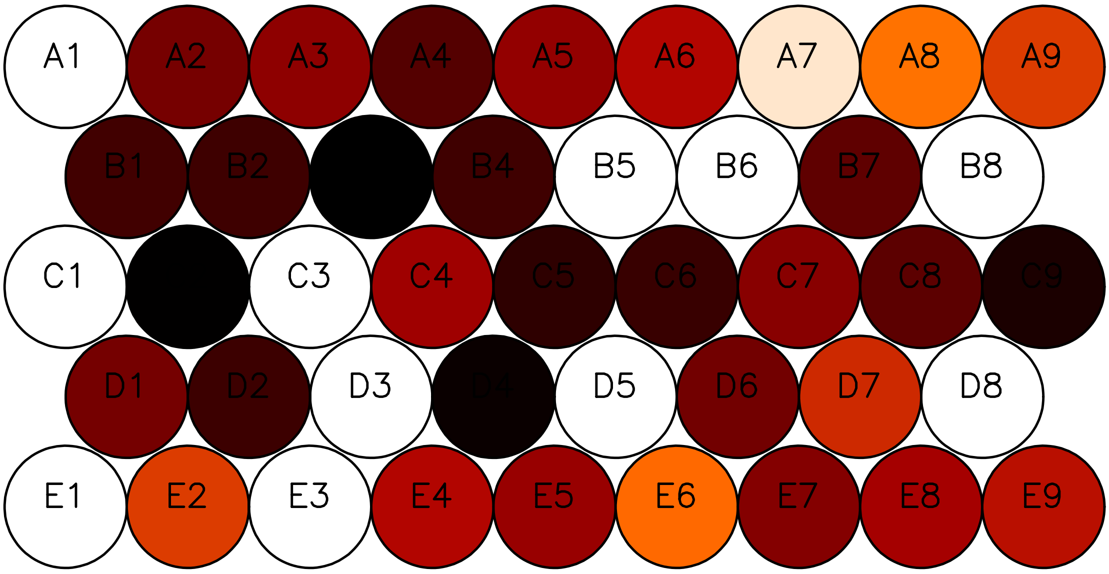

Figure 10: Case 3 - Image of distribution of excess power assuming bulk of load is from lid at 80 K.

3.1.4 Case 4: Lid at 197K

A loadcurve was taken at 05:18 on the 20th October (OBSID B00000BF). The actual temperature of the lid and shields during the measurement is shown in figure 11. In order to make the results as accurate as possible I have fitted the lid (PT1000_SPARE1) data and used the fit to generate the temperature of the lid at each point in the load curve. This means the estimate of the contribution from the lid can be assessed much more accurately. Figure 12 gives the results in the same format as for Case 1 except here the excess power is taken as the optical power incident on the SPIRE aperture excluding the estimated contribution from the lid (see appendix for how this was calculated). This power therefore represents the "stray" light that cannot be explained by the load from the mirrored reflector filling the beam. Note here that the two temperature based methods of estimating the power now agree and again the load curve power measurement as seems unreliable – further investigation into this is required.

Figure 13 shows the distribution of the straylight across the array. As with the PCAL flash row A (and possibly row E) appears to show increased straylight compared to the average across the array.

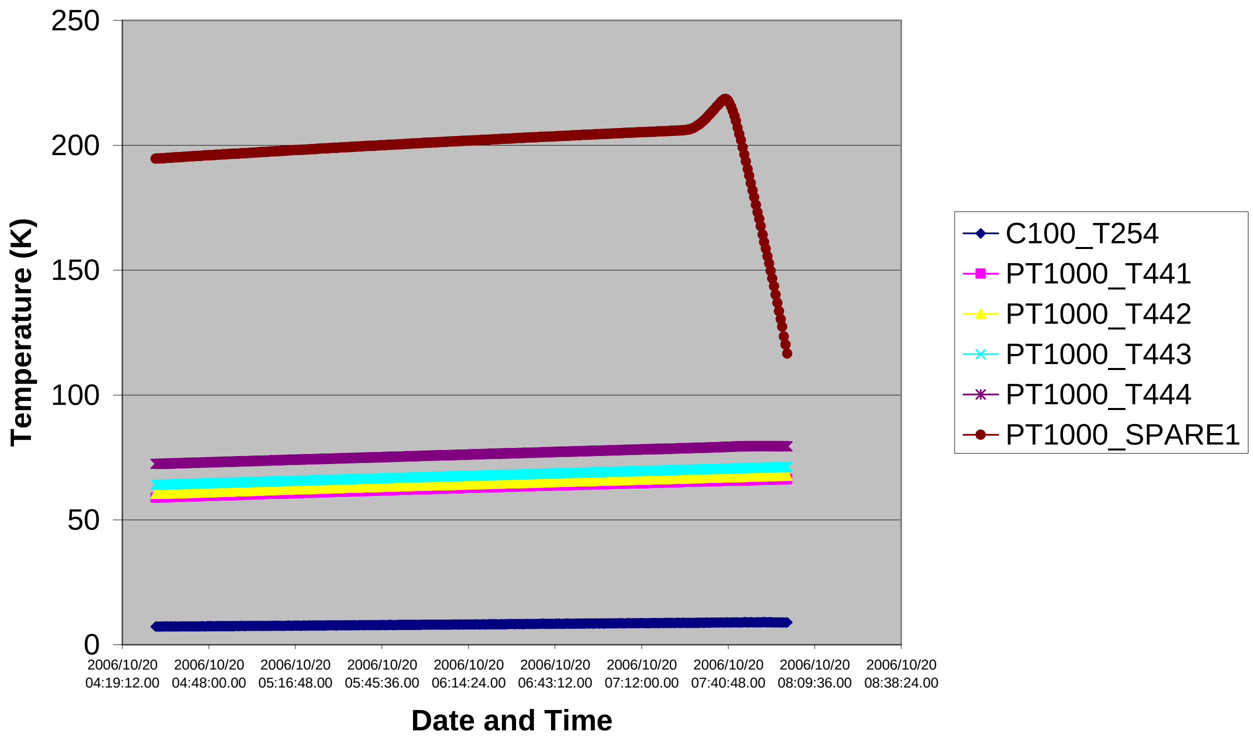

Figure 11: Lid and shield temperatures during case 4.

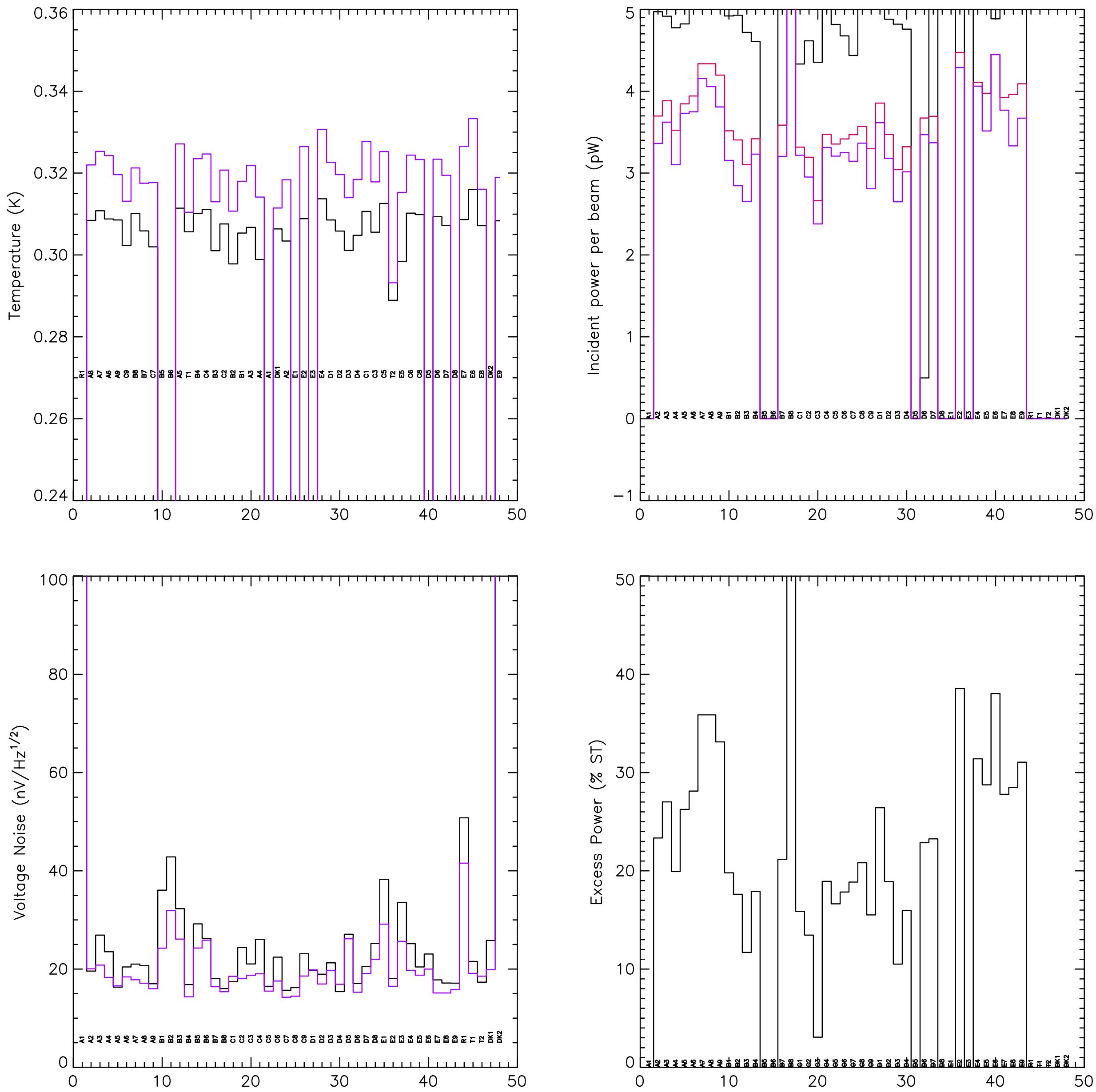

Figure 12: Results for Case 4/Case 2 comparison.

Upper left: Temperature. Case 2 black; Case 4 Purple.

Upper right: Estimated incident power on SPIRE calculated by the three methods described in the text. (i) Black; (ii) Red; (iii) Purple.

Lower left: Voltage noise at standard bias – Case 2 black; Case 4 Purple

Lower right: Excess incident power on SPIRE over and above that from the ~197K mirrored lid expressed as percentage of the "standard telescope".

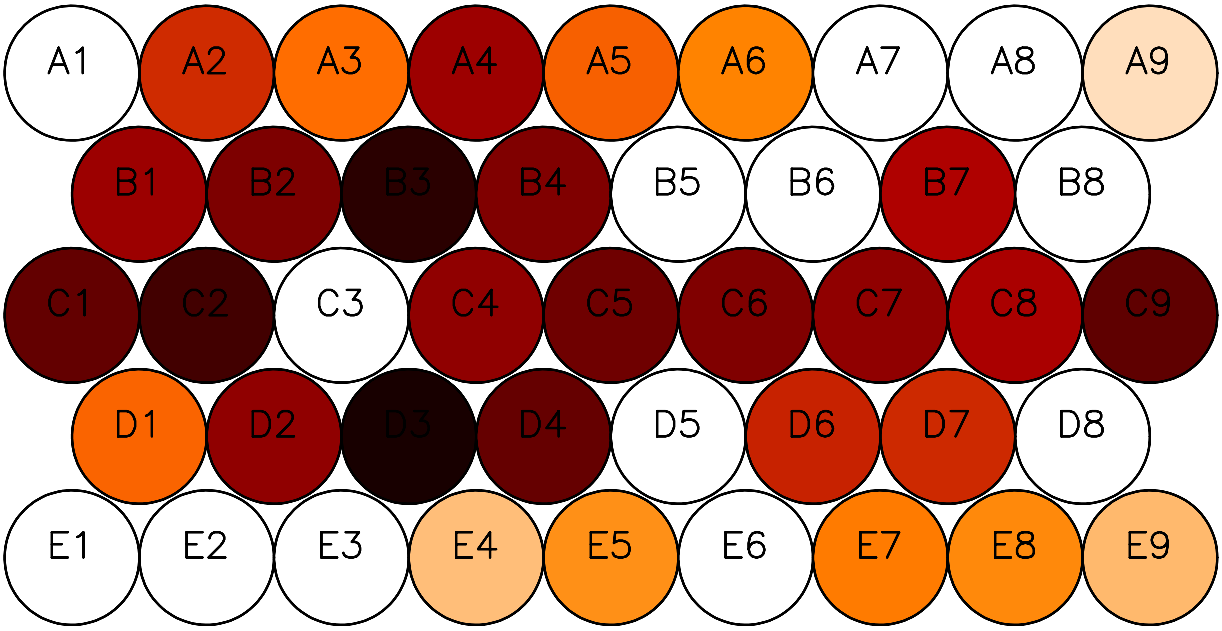

Figure 13: Case 4 - Image of distribution of excess power assuming bulk of load is from lid at 197 K.

3.1.5 Case 5: Cold Lid with Hot Shields

A loadcurve was taken at 09:25:17 on the 20th October when lid was below 10 K and the inner shields were set to the "hot" case (OBSID B00000C8). The actual temperature of the lid and shields during the measurement is shown in figure 14. As indicated in the caption T443 and T444 are on the second shield which was set close to 80K. T444 seems to give a rather different temperature compared to the others and requires further investigation. In this case the lid is cold and there is no need to take into account the direct load to elucidate the straylight level. Figure 15 gives the results in the same format as for Case 3 and Case 4 except here the excess power is the optical power incident on the SPIRE aperture directly with no need to account for the power from the lid. Note here that the two temperature based methods of estimating the power agree and I have left off the loadcurve power comparison

Figure 16 shows the distribution of the straylight across the array. All edges appear to show increased straylight compared to the average across the array. Once again the B8 result is anomalous.

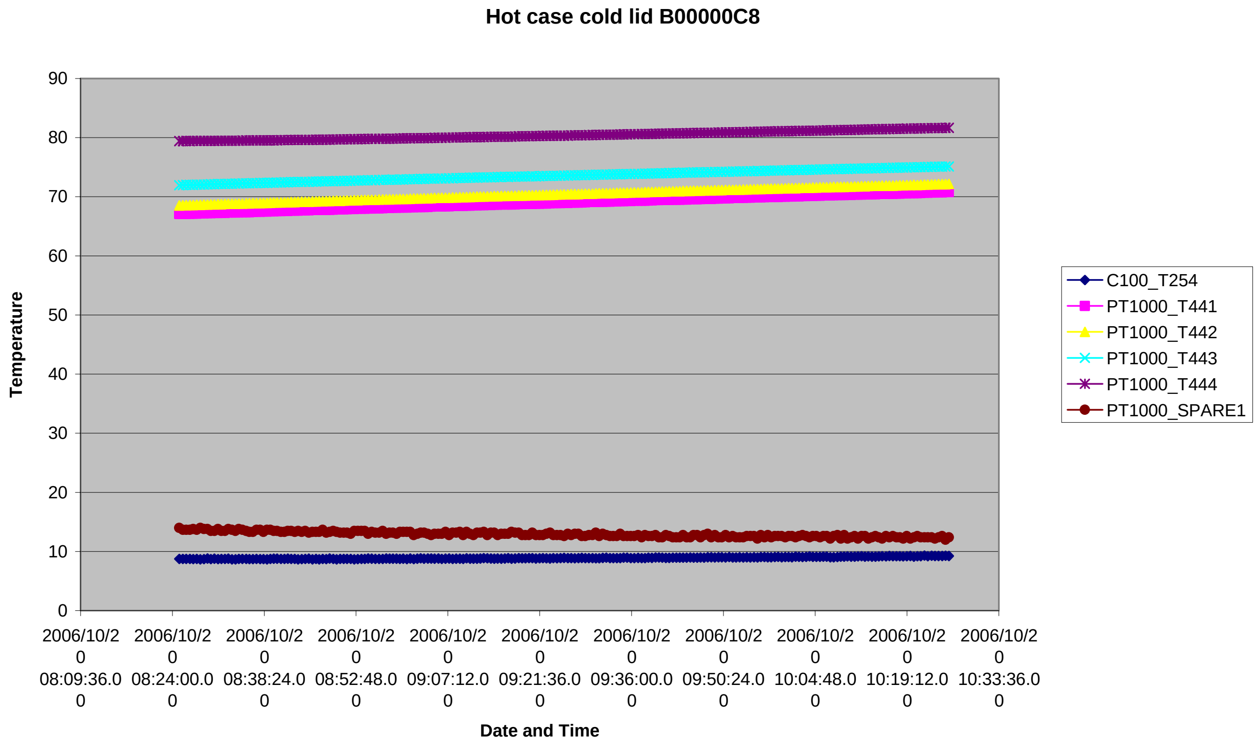

Figure 14: Lid and shield temperatures during case 5. Thermistors T443 and T444 are mounted on the second shield. T444 is close to the optical beam.

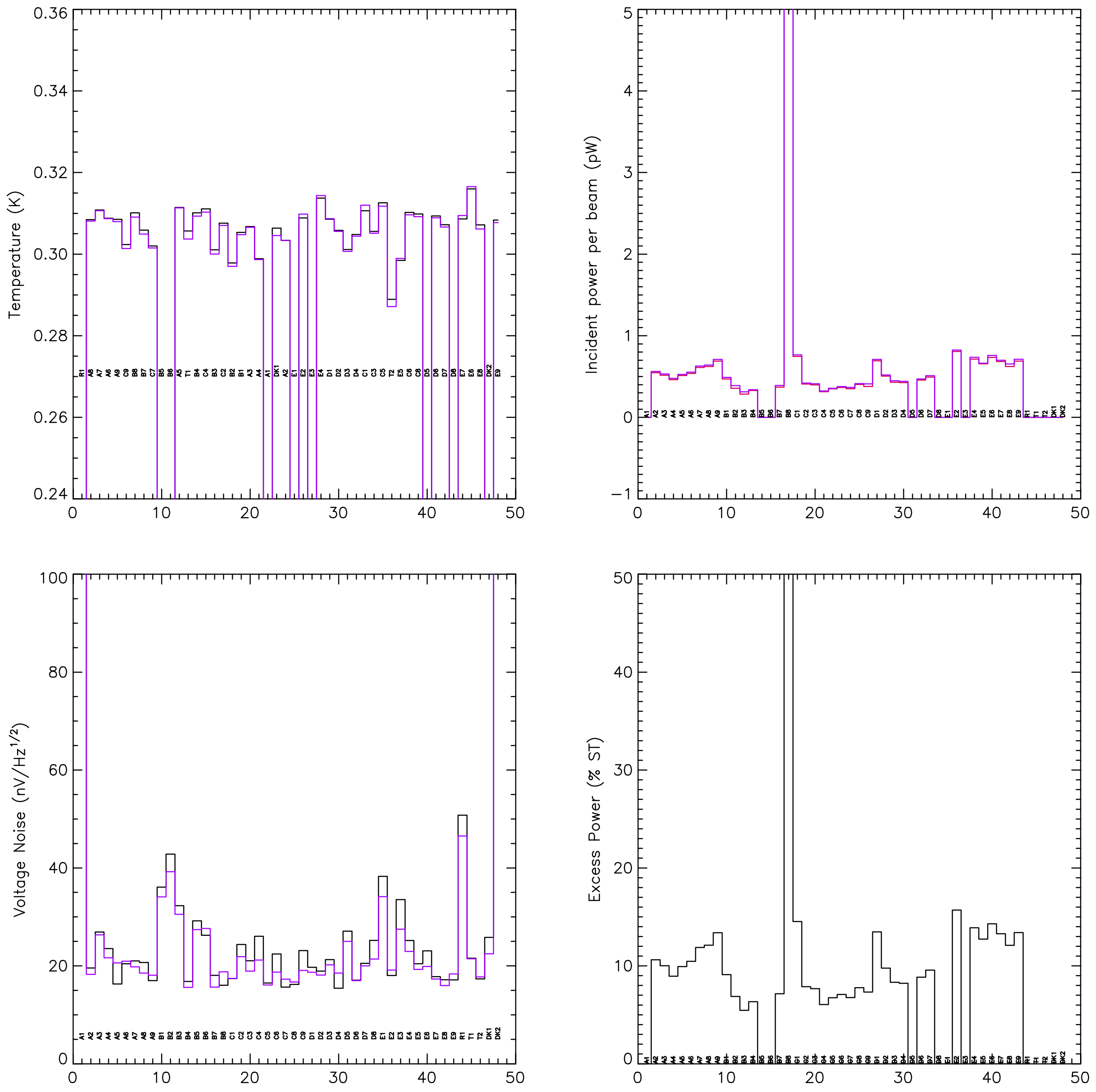

Figure 15: Results for Case 5/Case 2 comparison.

Upper left: Temperature. Case 2 black; Case 5 Purple.

Upper right: Estimated incident power on SPIRE calculated by the two methods described in the text. (ii) Red; (iii) Purple.

Lower left: Voltage noise at standard bias – Case 2 black; Case 5 Purple

Lower right: Incident power on SPIRE expressed as percentage of the “standard telescope”.

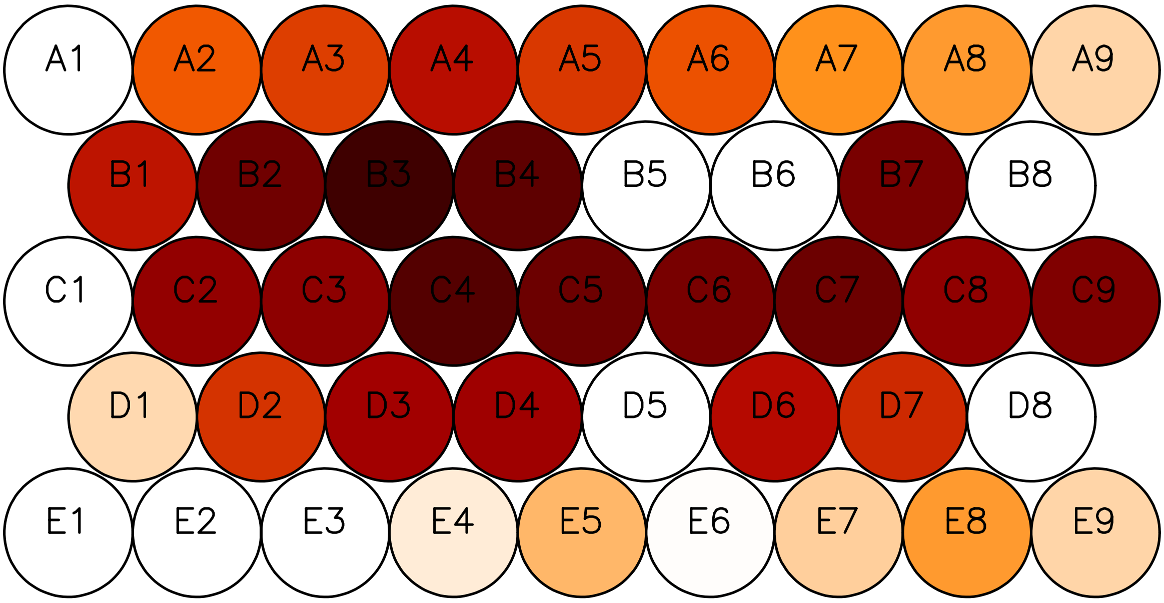

Figure 16: Case 5 - Image of distribution of excess power across the array

3.2 External Illumination Tests

The processing of the chopped external source data as slightly different from the static tests. The first part is the same and I convert the signal into estimated power using comparison to the temperature at the same bias setting during the cold load curve (Case 2 above). From the time series of estimated power during the time the source was exposed, I have removed the baseline drift using a low order polynomial and transformed to the frequency domain to attempt to find the chopped signal from the source. In two cases (1 and 2) a clear signal at the chopper frequency was seen and it was possible to estimate the power incident on the SPIRE aperture due to the source alone. The results are reported below for each case in table 2

3.2.1 Case 1: External source aligned on LOU port

Figure 17 shows the power spectrum for each pixel in the array zoomed in to the region around the 1.7 Hz chop frequency. The chop signal is very clearly identified and it is possible to estimate the power from the source from the peak of the spectrum at around 1.7 Hz. This is indicated in figure 17 as a red star.

Figures 18 and 19 show the peak of the power spectrum at 1.7 Hz as a function of pixel in the array as raw power and as percentage of the standard telescope. Figure 20 shows the distribution of the power across the array. The apparently large response in pixel D6 is due to it being noisy – see PSD in figure 17.

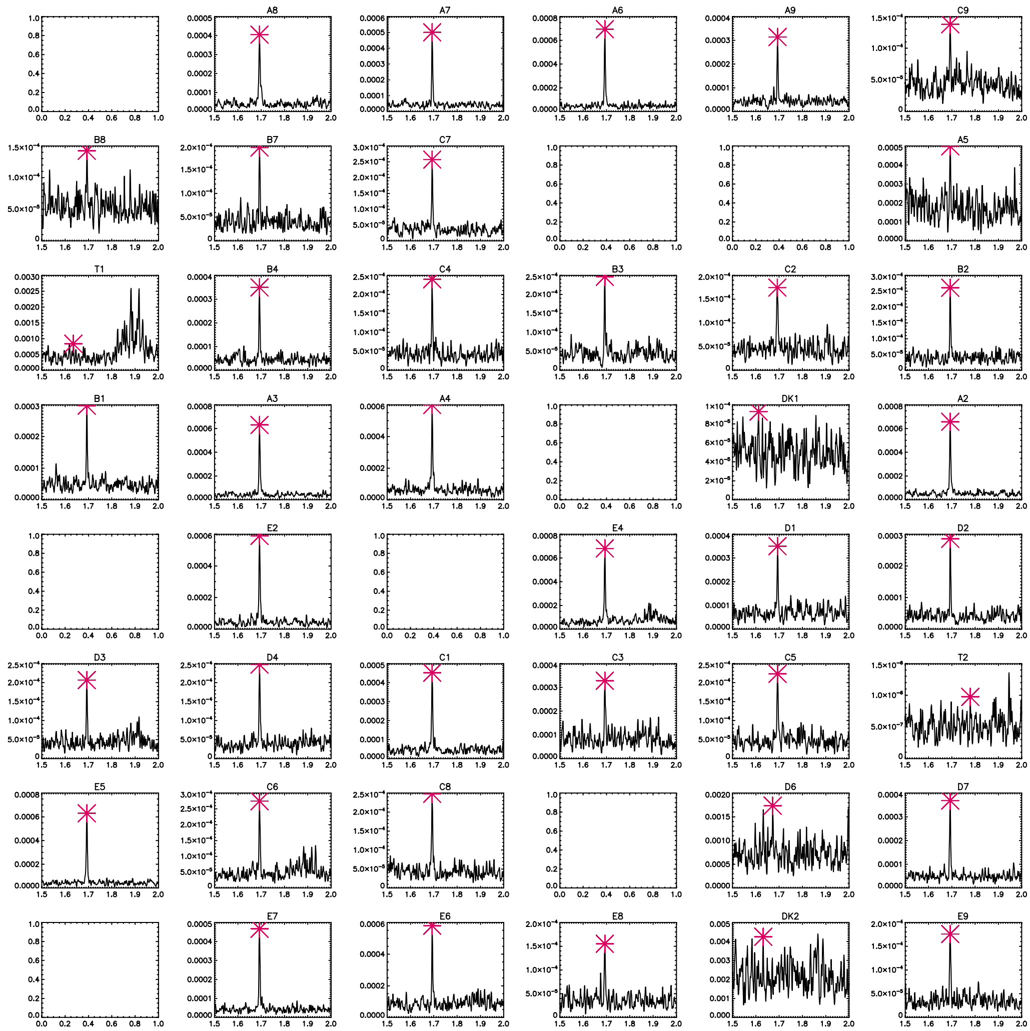

Figure 17: Case 1 Power (in pW) versus frequency (in Hz) for each channel in the array – non operational channels are blank. The red star indicates the maximum in the 1.6 to 1.8 Hz region

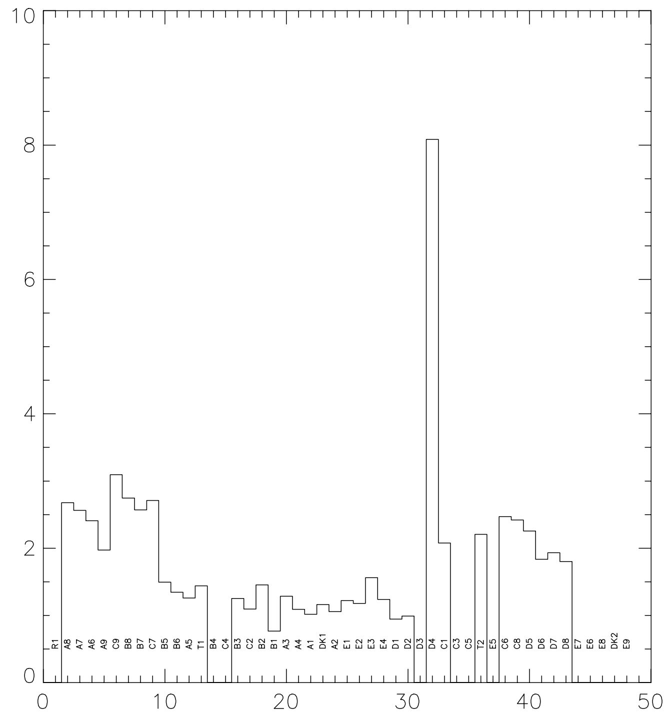

Figure 18: Chopped Case 1: The 1.7 Hz peak power per pixel in femtowatts (fW). Ignore the pixel labelling as it is incorrect – *to be fixed in next version.*

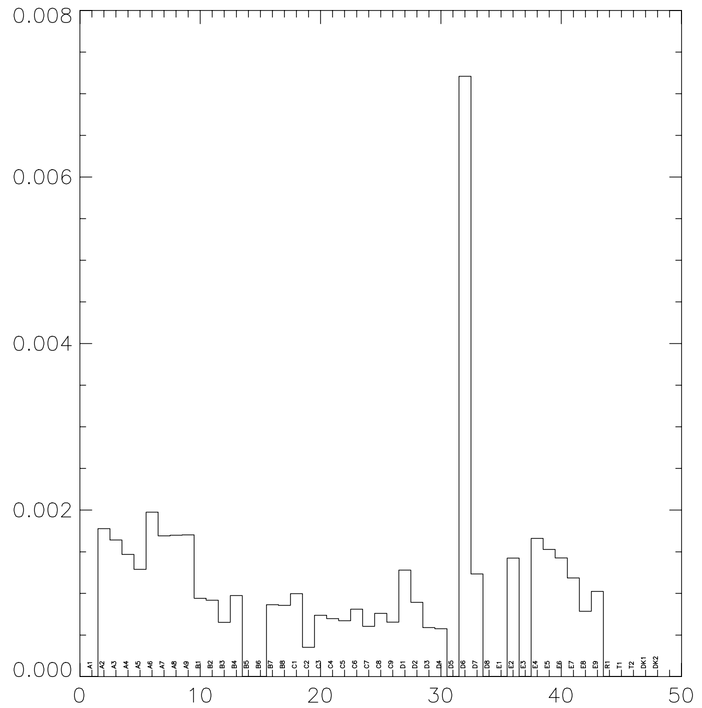

Figure 19: Chopped Case 1: The source Power incident on SPIRE aperture per pixel expressed as percentage of standard telescope

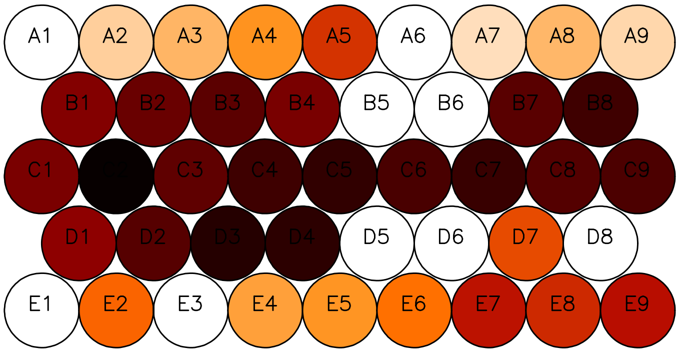

Figure 20: Chopped Case 1: Power distribution across the array

3.2.2 Case 2: External Source at +15 mm with respect to LOU

The chopped signal was detected in the power spectra again and figures 21 through 23 show the results for Case 2 in the same way as for Case 1, except I have left out the raw power versus pixel plot.

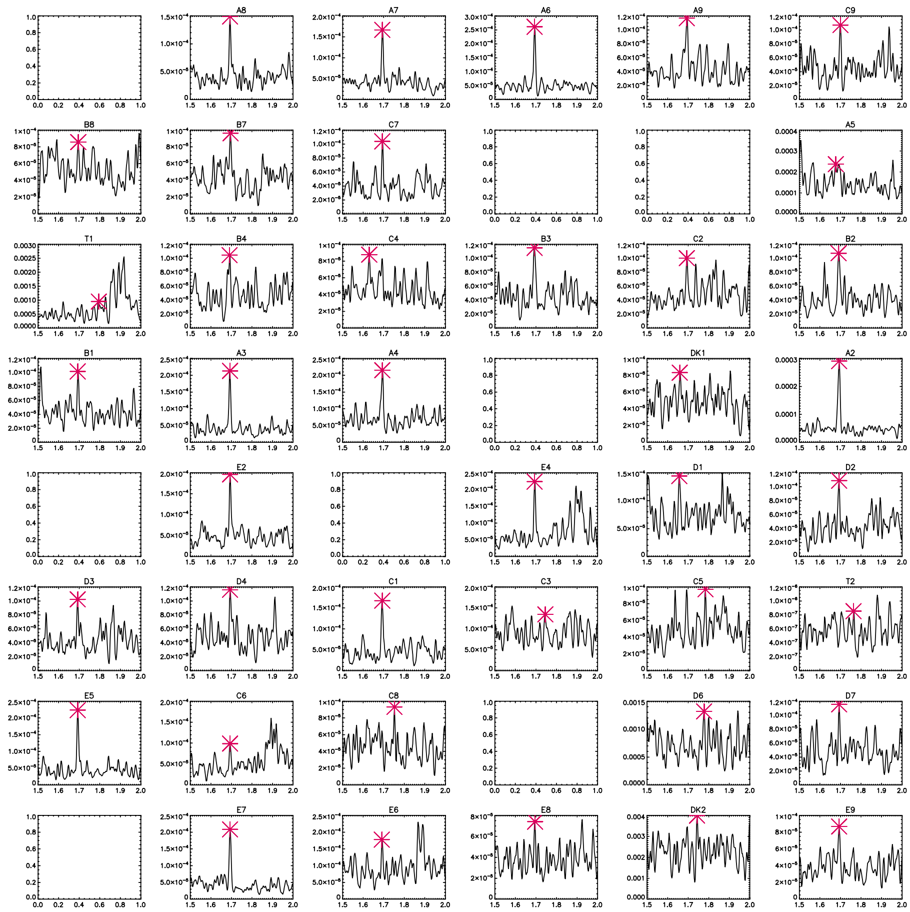

Figure 21: Chopped Case 2: Power (in pW) versus frequency (in Hz) for each channel in the array – non operational channels are blank. The red star indicates the maximum in the 1.6 to 1.8 Hz region

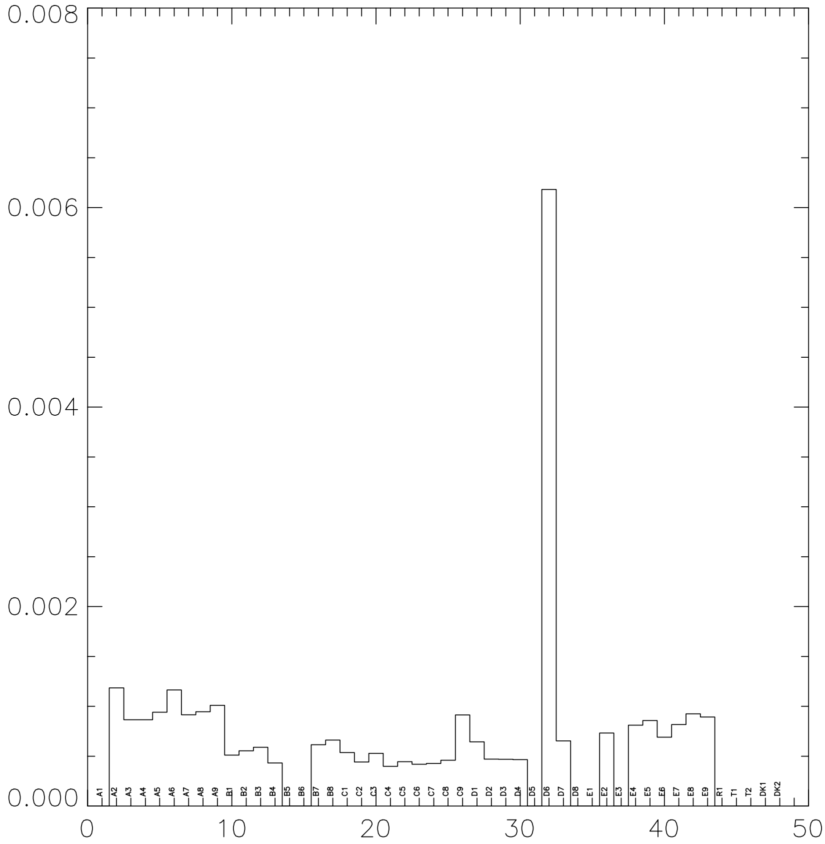

Figure 22: Chopped Case 2: The source Power incident on SPIRE aperture per pixel expressed as percentage of standard telescope

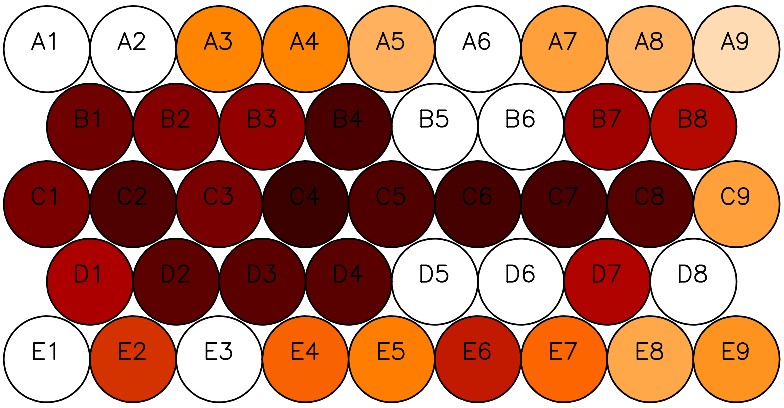

Figure 23: Chopped Case 1: Power distribution across the array

3.2.3 Case 3: External source at LOU +30 mm

No signal was observed in the power spectra

3.2.4 Case 4: External source at LOU – LOU blocked with tape

No signal was observed in the power spectra

3.2.5 Case 5 and 6: External source at alignment windows

No signal on either

4 Summary of Results and Comparison to Model

Table 3 collects the average results from both the static and chopped tests and gives a first cut comparison to the Astrium model from the spreadsheet. For comparison where results are in Watts, the in band power from the "standard" telescope (ST) is expected to be 5.1×10^{-12} W. The results from the Astrium spreadsheet are hard to understand and I have done my best to understand them but it is not clear what the temperature of the shields is for all the cases.

Case	Cryostat set up	Average detected power across FOV	Expected from Model	Comments
Static 0,1,2	Cold lid cold shield	No detectable signal greater than ~2×10^{-14} W	No Prediction?	At limit of temperature calibration and comparison method for CQM.
Static 3	Warm lid ~80 K	3.5-5 % of ST	No Prediction	Up to 10% of ST at edges of FOV
Static 4	Hot lid ~ 197 K	18-20 % of ST	No Prediction	Up to 30-35% of ST at edges of FOV
Static 5	Cold lid with warm shields	6-8 % of ST	~8 % of ST?	Up to 10-15% of ST at edges of FOV
Chopped 1	HBB centred on LOU band 3 port - this is Z_o	0.8-1×10^{-3} % of ST	0.13×10^{-3} % of ST	Up to 2-3 $\times10^{-3}$ % of at edges of FOV
Chopped 2	HBB moved Z_o+15 mm wrt LOU port	0.5-0.7×10^{-3} % of ST	A bit lower than above?	Up to 1 $\times10^{-3}$ % of at edges of FOV
Chopped 3	HBB moved Z_o+30 mm wrt LOU port	No detectable signal greater than ~5×10^{-16} W	N/A	No peak in PSD at chop frequency – limit set by approximate level of noise and systematics
Chopped 4	LOU port blocked with tape	No detectable signal greater than ~5×10^{-16} W	N/A	No peak in PSD at chop frequency – limit set by approximate level of noise and systematics
Chopped 5	HBB centred on left alignment port	No detectable signal greater than ~5×10^{-16} W	No prediction	No peak in PSD at chop frequency – limit set by approximate level of noise and systematics
Chopped 6	HBB centred on right alignment port	No detectable signal greater than ~5×10^{-16} W	No Prediction	No peak in PSD at chop frequency – limit set by approximate level of noise and systematics

Table 3: Summary of results and comparison with the predictions from the Astrium model (as far as I can understand them)

Inspection of table 3 shows that the measured and predicted (where available) are in reasonable agreement except for the prediction for the HBB though the LOU where the measurement is 5-10 higher than the prediction. Given the difficult nature of the measurement; the low level of the both prediction and measurement and my lack of knowledge of the model parameters this is probably acceptable.

Final conclusion: Cryostat straylight is within specification for SPIRE.

Appendix: Emissivity of the Aluminium Reflector

The theoretical emissivity of a metal (high conductivity) surface is given by

$$\varepsilon = 4Z/Z_o$$

where Z is surface impedance and Z_o the impedance of free space (367.7 Ω). In convenient units the surface impedance can be written as:

$$Z = 0.199 \sqrt{(\rho\nu)} \quad \Omega$$

Where ρ is the optical frequency in THz and ρ the bulk resistivity in 10^{-8} Ω m. Using the bulk resistivity vlues for pure aluminium gives a rather low emissivity for the cryostat cover mirror at 80 K ($\varepsilon \sim 0.08$) leading to a large contribution from "straylight" to the gross load in the static cases described in the main case. We should rather use the bulk conductivity appropriate to aluminium alloy which will be rather higher than the pure metal. Although we (I!) don't know the actual composition of the alloy used in the mirror, most alloys have a copper content of ~2%. Macchioni, Rayne and Bauer (Phys Rev B **25** 1982) give measured bulk resistivity values for various aluminium-copper alloys and I have used data from this paper to deduce the emissivity of the cryocover mirror. The values I use in the calculations are as follows:

$$\varepsilon(197K) = 0.229$$
$$\varepsilon(80K) = 0.132$$

Using these values gives a much more reasonable value for the straylight component in the cases described in the body of the report.